

ZippyPoint: Fast Interest Point Detection, Description, and Matching through Mixed Precision Discretization

Simon Maurer*, Menelaos Kanakis*, Matteo Spallanzani, Ajad Chhatkuli, and Luc Van Gool

Abstract—The design of more complex and powerful neural network models has significantly advanced the state-of-the-art in local feature detection and description. These advances can be attributed to deeper networks, improved training methodologies through self-supervision, or to the introduction of new building blocks, such as graph neural networks for feature matching. However, in the pursuit of increased performance, efficient architectures that generate lightweight descriptors have received surprisingly little attention. In this paper, we investigate the adaptations neural networks for detection and description require in order to enable their use in embedded platforms. To that end, we investigate and adapt network quantization techniques for use in real-time applications. In addition, we revisit common practices in descriptor quantization and propose the use of a binary descriptor normalization layer, enabling the generation of distinctive length-invariant binary descriptors. ZippyPoint, our efficient network, runs at 47.2 *fps* on the Apple M1 CPU. This is up to $5\times$ faster than other learned detection and description models, making it the only real-time learned network. ZippyPoint consistently outperforms all other binary detection and descriptor methods in visual localization and homography estimation tasks. Code and trained models will be released upon publication.

I. INTRODUCTION

The detection and description of geometric regions in images, such as salient points or lines, is one of the fundamental components for geometric computer vision tasks such as Simultaneous Localization and Mapping (SLAM) and Structure-from-Motion (SfM). Deep neural networks (DNNs) have significantly advanced the representational capability of descriptors by learning on large scale natural images [1], using deeper networks [2], or introducing new modules to learn feature matching [3]. However, these advances often come at the cost of more expensive models with slow run times, and large memory requirements for storage. While the demand for real-time applications such as autonomous driving, robotics, and augmented reality is increasing, methods that can operate in real-time on computationally limited platforms have received surprisingly little attention.

Systems that need high-quality image correspondences include autonomous cars, Unmanned Aerial Vehicles (UAVs),

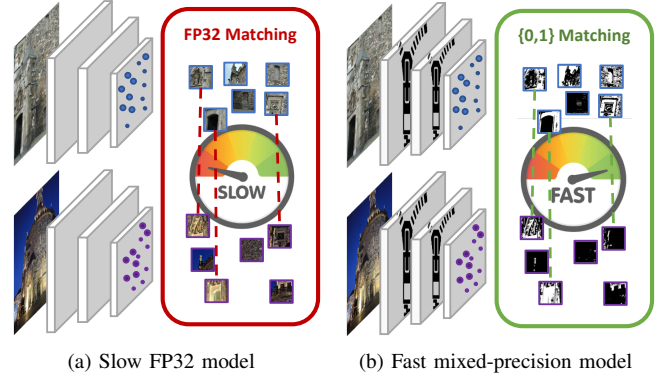


Fig. 1: Learned detection and description methods are often slow at inference and generate floating point descriptors that are slow to match (a). In this paper we present ZippyPoint (b), a real-time detection and description network, running $5\times$ faster than other learned alternatives on a CPU and provide binary descriptors for fast and efficient matching.

and augmented reality glasses, to name a few. A key component to their success in large-scale applications is the real-time extraction of binary descriptors. This not only enables efficient storage of the detected representation, e.g. the map in SLAM pipelines, but also accelerated descriptor matching. Fast and light weight descriptor methods include BRISK [4], BRIEF [5] and ORB [6], however, their matching capability is often inferior to standard hand crafted features such as SIFT [7] and SURF [8], as presented by Heintz J. *et al.* [9]. In challenging real-life scenarios, however, hand-crafted feature extractors are outperformed significantly by learned representations [10]. While the performance gains of learned methods are highly desired, embedded platforms are limited in storage, memory, providing limited or no support for floating-point arithmetic, thus rendering the use of learned methods infeasible.

Motivated by the desire for learned method performance on embedded platforms, we explore network quantization to let DNNs operate under such challenging constraints. The quantization of a DNN is not as straightforward as selecting the discretization level of convolutional layers, however. Quantized DNNs often require different levels of discretized precision for different layers [11], [12]. Operations such as max-pooling favour saturation regimes [11], and average pooling is affected by the required rounding and truncation operations. In addition, prior works often focus on image-level classification tasks, with findings that do not necessarily transfer to new tasks [13]. In addition, besides being real-time, the DNN needs to additionally generate binary local descriptors for storage efficiency and fast feature matching.

*S. Maurer, and M. Kanakis contributed equally to this work.

S. Maurer, M. Kanakis, and A. Chhatkuli are with the Computer Vision Lab, ETH, Zurich 8092, Switzerland (e-mail: simomaur@protonmail.com; menelaos.kanakis@vision.ee.ethz.ch; ajad.chhatkuli@vision.ee.ethz.ch).

M. Spallanzani is with the Integrated Systems Laboratory, ETH, Zurich 8092, Switzerland (e-mail: spmatteo@iis.ee.ethz.ch).

L. Van Gool is with the Computer Vision Lab, ETH, Zurich 8092, Switzerland, and also with the Katholieke Universiteit Leuven, Leuven 3000, Belgium (e-mail: vangool@vision.ee.ethz.ch).

This adds further challenges, since the discretization of the output layer draws less precise boundaries in the feature domain [14], making the network optimization more challenging. Furthermore, prior works focus on global feature description and present findings that do not trivially transfer to our task [15], [16].

To render the search for a Quantized Neural Network (QNN) tractable, we propose a *layer partitioning and traversal* strategy, significantly reducing the architecture search complexity. Specifically, we partition the DNN layers into groups, which we refer to as Macro-Blocks. We identify the best performing operation or quantization precision for the first upstream block. We then sequentially traverse downstream through the remaining macro-blocks, selecting the optimal setting for each, one at a time. While most research considers homogeneous quantization precision across all layers, we reach better results using mixed-precision quantization [12]. In addition, we find that replacing standard pooling operations with learned alternatives can improve QNN performance. For the binarization of descriptors, we revisit the metric learning methodology and introduce a normalization layer that constrains the representation to a pre-defined number of bits. The binary normalization layer is therefore analogous to the L_2 normalization used for continuous vectors.

We demonstrate the generality of our proposed QNN with binary descriptors, coined ZippyPoint (Fig. 1), on two different tasks. First, we conduct thorough experiments on Homography Estimation, a common test case in learned descriptor methods. To further evaluate the usability of ZippyPoint in real-life applications, we also report the performance on Camera Localization, an essential task for SLAM and SfM pipelines. In summary, our contributions are:

- We propose a heuristic algorithm, named *layer partitioning and traversal strategy*, to investigate the topological changes required for the quantization of a state-of-the-art detection and description network. We find that with a mixed-precision quantization architecture we can achieve a $5\times$ speed-up with minor performance degradation. This demonstrates that the usual homogeneous quantization, or the use of max pooling, can be sub-optimal.
- We propose the use of a normalization layer for binary descriptors. Our normalization layer enables the end-to-end optimization of binary descriptors. Incorporating the normalization layer yields consistent improvements.
- We present ZippyPoint, the first learned detection and description network that can operate in real-time on an Apple M1 CPU. ZippyPoint consistently outperforms all real-time CPU methods for visual localization and homography estimation, while significantly decreasing the storage requirements for the sparse map.

II. RELATED WORK

Hand crafted feature extractors The design of hand-crafted sparse feature extractors such as SIFT [7] and SURF [8] has been quite successful. While still widely

used in applications such as SfM [17], the time needed for descriptor extraction, coupled with their floating-point representation, limits them from being used in computationally constrained and embedded platforms such as light-weight UAVs. Motivated by this limitation, methods like BRISK [4], BRIEF [5], and ORB [6], aimed to provide fast and compact features targeted for real-time applications [18]. While fast and lightweight, they often lack the representational strength to perform well under camera view changes [9], [17].

Learned feature extractors Advances in deep learning have enabled the learning of robust, (pseudo-)invariant, and highly descriptive image features, pushing the boundaries of what was previously possible through handcrafted methods. Recent efforts have also brought the aforementioned advantages of learning methods to local image point features. While hand-crafted local features [7], [8], [4], [5], [6], [20] have not evolved much, systematic incremental progress can be seen in the learned local features [21], [1], [22], [23], [24], [19], [2]. Improvements have been achieved using contrastive learning [21], self-supervised learning [1] and optimized architectures [24], [19] to name a few approaches. Nevertheless, time and memory inefficiency remain major drawbacks of the learned methods.

In the same vein, large scale descriptor matching calls for light-weight representations. Binary descriptors enable efficient matching with moderate performance drops while significantly decreasing the storage requirements. Yet, the existing literature on quantization and binary representations focuses on image retrieval [25], [15], [16], [26], [27], [28], neglecting the detection and description of local features. For descriptor binarization, [15], [26], [25] use multistage optimization procedures. More similar to our work, [28] defines a differentiable objective for the hamming distance. Meanwhile, [16] uses sigmoids to soften the optimization objective, enabling end-to-end optimization of the neural network and the descriptor without the need for multiple optimization steps. In the same spirit, we optimize the network in a single optimization step as in [28], [16]. Moreover, we argue that the lack of normalization layer that is a staple in metric learning [29], greatly hinders the descriptor performance. We, therefore, propose a binary normalization layer, drawing inspiration from declarative networks [30], that enables end-to-end optimization without requiring the use of gradient approximations of multiple optimization stages.

Efficient Neural Networks Several solutions have been proposed to deploy neural networks in constrained scenarios. These solutions can be partitioned in topological optimizations, aiming at increasing accuracy-per-operation or accuracy-per-parameter [31], [32], software optimizations such as tensor decomposition and parameter pruning [33], [34], [35], and hardware-aware optimizations [11].

Amongst hardware-aware optimizations, quantization plays a central role [11], [12]. By replacing Floating-Point (FP) with Integer (INT) operands, a QNN can reduce its storage and memory requirements with respect to an architec-

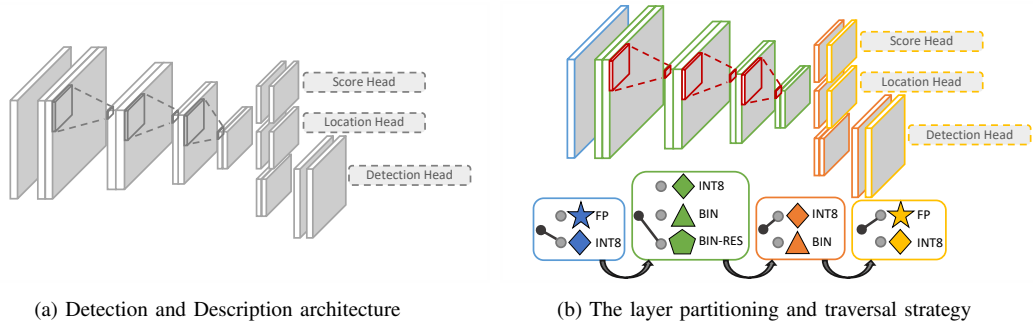


Fig. 2: (a) Starting from [19], we partition the operations in macro-Blocks, depicted in (b) with different colors. From the first upstream macro-Block, in blue, we identify the optimal quantization setting that maintains functional performance while improving the network’s throughput. We then traverse to the next block, green, and repeat. The strategy is complete once we have reached the most downstream network layer, the prediction heads.

turally equivalent DNN. In addition, complex FP arithmetic can be replaced by simpler INT arithmetic. Due to these properties, QNNs can be executed at higher throughput (number of operations per cycle) and arithmetic intensity (number of arithmetic operations per memory transaction) than equivalent full-precision DNNs [36]. When operand precision is extremely low (e.g., binary), standard instruction set architectures can be exploited to increase these metrics even further [11]. With respect to mainframes and workstations, embedded platforms have limited storage and memory, limited or no support for FP arithmetic, and are optimized to execute single instruction, multiple data (SIMD) integer arithmetic. These considerations make QNNs an ideal fit for embedded applications, where latency constraints are often critical.

However, QNNs have limited representational capacity compared to their FP counterparts. Specifically, linear operations using discretized weights draw less precise boundaries in their input domains. In addition, discretized activation functions lose injectivity with respect to their FP counterparts, making quantization a lossy process [14]. To mitigate such functional drops, [12] decompose the quantized feature extraction layers into two additive branches, a lower-precision branch modelling coarse-grain information, and a higher-precision branch modelling fine-grain information. This solution, however, comes at the cost of requiring casting operations to combine the results of lower- and higher-precision branches, and therefore increases latency.

These conflicting properties make the identification of optimal quantization policies a multi-objective problem. On the one hand, low-precision policies can maximise hardware fitness and suitability for constrained (e.g., real-time) applications. On the other hand, higher-precision policies can better preserve a network’s functionality.

III. MIXED PRECISION DISCRETIZATION

Efficiently identifying salient points in images and encoding them with lightweight descriptors is key to enabling real-time applications. In this paper, we explore the efficacy of learning-based descriptor methods under two constraints: minimizing run-time latency and using binary descriptors. In Sec. III-A we introduce the baseline architecture we initiate

our investigation from. In Sec. III-B we propose a strategy to explore structural changes to the network, aiming at accelerating inference. In Sec. III-C we introduce a standard formulation of metric learning, which we use to define our binary descriptor normalization layer.

A. Baseline Architecture

We initiate our investigation from the state-of-the-art KP2D [19] network, which is similar to the parallel work of [24]. The KP2D model maps an input image $I \in \mathbb{R}^{H \times W \times 3}$ to keypoints $\mathbf{p} = \{[u, v]\} \in \mathbb{R}^{N \times 2}$, descriptors $\mathbf{f} \in \mathbb{R}^{N \times 256}$, and keypoint scores $\mathbf{s} \in \mathbb{R}^N$, where N represents the total number of keypoints extracted. The model is comprised of an encoder with 4 VGG-style blocks [37], followed by a three-headed decoder for keypoints, keypoint scores, and descriptors. The distinction between encoder and decoder is decided by the reduction of or increase in the spatial resolution of the input. The encoder is therefore comprised of 8 convolutions, the keypoint and keypoint score branches of 2, and the descriptor branch of 4. All convolutional operations, except for the final layers, are followed by batch normalization and leaky rectified linear hidden units (leaky ReLUs) [38]. The model is optimized through self-supervision by enforcing consistency in predictions between a source image I_s and a target image $I_t = \mathbf{H}(I_s)$, related through a known homography transformation \mathbf{H} and its warping function \mathbf{H} .

We chose KP2D as the starting point for our investigation as it follows standard architecture design choices: a VGG style encoder [1], [39], [2], [24], encoder-decoder structure [1], [39], and the detection and description paradigm [1], [39], [2], [24]. Therefore, we expect that the investigated quantization strategy can transfer to other similar models, such as the ones listed above.

B. Network Quantization

For the quantization of a convolutional layer, several additional design choices are required, such as weight precision, feature precision, and whether to use a high precision residual. When considering whole networks, this consideration leads to a combinatorially large search grid, rendering an exhaustive search of the ideal quantization policy prohibitive.

To simplify the search space, we propose a layer partitioning and traversal strategy, depicted in Fig. 2. First, we partition the operations of our target architecture into macro-blocks. For each macro-block, we define a collection of candidate quantized configurations. We then traverse through the macro-blocks and identify the optimal configuration for each, one at a time. This heuristic algorithm terminates once we have reached the most downstream network layer, the prediction heads. Note that, while we maintain the macro-block configurations the same once selected, the architecture is optimized end-to-end. This strategy reduces the search complexity from combinatorial (the product of the number of configurations for each macro-block) to linear (the sum of the number of configurations for each macro-block). In addition, it ensures that when a macro-block is optimized on features with given representation capabilities, it will not degrade due to optimization of a different macro-block upstream. We detail our choice of macro-blocks and their configurations in the experiments section.

C. Binary Learned Descriptors

Preliminaries When describing an image or a local patch, the learned mapping aims to project a set of data points to an embedding space, where similar data are close together and dissimilar data are far apart. A fundamental component to the success of learned descriptors is the advancement of contrastive losses [40], [41], [42]. To ensure stable optimization and avoiding mode collapse, embeddings are often normalized [29]. A common selection is L_2 normalization, defined as

$$y = \frac{1}{\|x\|_2} x. \quad (1)$$

While the solution, and hence gradients, can be expressed in closed-form, it is inapplicable in the case of binary descriptors. Specifically, binary descriptors can take values 0,1, with unit length indicating a one hot vector. Therefore, we rewrite the normalization layer as an generalized optimization objective

$$\begin{aligned} y = \arg \min_{u \in \mathbb{R}^n} \quad & \text{sim}(u) \\ \text{subject to} \quad & \text{constr}(u). \end{aligned} \quad (2)$$

Equation (2) is equivalent to equation (1) if we substitute the $\text{sim}(u) = \frac{1}{2}\|u - x\|_2^2$ and $\text{constr}(u) = \|u\|_2 = 1$. This enables the definition of optimization objectives that can be utilized where L_2 normalization does not provide the required behaviour. While optimization objectives are not differentiable, their use if made possible through advances in deep declarative networks [30].

Normalization for Binary Descriptors We hypothesize that normalization for binary descriptors is equivalent to having a constant number of ones. To this end, we take inspiration from multi-class classification problems and view the binary normalization as a projection of the descriptors living in an n -dimensional hypercube on a k -dimensional polytope [43]. In other words, an n -dimensional descriptor has entries that sum

to k . This trivially defines the constraint from equation (2) to $\text{constr}(u) = 1^\top u = k$.

We define the new optimization objective as

$$\begin{aligned} y = \arg \min_{0 \leq u \leq 1} \quad & -x^\top u - H(u) \\ \text{subject to} \quad & 1^\top u = k \end{aligned} \quad (3)$$

where $H(u)$ is the binary cross entropy function.

To optimize the objective, we introduce a dual variable $\nu \in \mathbb{R}$ for the constraint of equation (3). The Lagrangian then becomes

$$-x^\top u - H(u) + \nu(k - 1^\top u), \quad (4)$$

Differentiating with respect to u , and solving for first-order optimality

$$\begin{aligned} -x + \log \frac{u^*}{1 - u^*} - \nu^* &= 0 \\ u^* &= \sigma(x + \nu^*), \end{aligned} \quad (5)$$

where σ denotes the logistic function. We identify the optimal ν^* by using the bracketing method of [43] that is efficiently implemented for use on GPUs, and backpropagate using [44].

The selection of the optimization objective in equation (3) is two-fold. The use of the entropy regularizer helps prevent sparsity in the gradients of the projection. In addition, the forward pass, as seen in equation (5), boils down to an adaptive sigmoid given the descriptor. This enables the direct comparison with the common practice of approximating binary entries using the sigmoid function.

IV. EXPERIMENTS

We first present the implementation details in Section IV-A. In Section IV-B we conduct the layer partitioning and traversal strategy for the network quantization, as well as evaluate the proposed descriptor binarization. We finally combine the two contributions into ZippyPoint and evaluate its performance on the task of homography estimation. To demonstrate the generality of our model, Section IV-C presents the results on visual localization, evaluating the descriptor suitability on one of its most important applications. Code and trained models will be released upon publication, with the hope that it can spark further research in the design of binary descriptors and quantized networks for the task of keypoint detection and description.

A. Implementation Details

We implement our models in TensorFlow [45], and use the Larq [46] library for binary quantization. Our models are trained on the COCO 2017 dataset [47], comprised of 118k training images, following [1], [39], [19].

The models are optimized using ADAM [48] for 50 epochs with a batch size of 8, starting with an initial learning rate of 10^{-3} while halving it every 10 epochs. To ensure robustness in our results, we optimize each model configuration three times and report mean and standard deviation.

TABLE I: Results from the layer partitioning and traversal strategy. The final model, in bold, performs comparably to the baseline while running $5\times$ faster. Green highlights the configuration used in the next stage.

	Repeat. \uparrow	Loc. \downarrow	Cor-1 \uparrow	Cor-3 \uparrow	Cor-5 \uparrow	M.Score \uparrow	FPS \uparrow
KP2D [19]	0.686	0.890	0.591	0.867	0.912	0.544	9.5
Baseline (ours)	0.649 ± 0.004	0.792 ± 0.015	0.566 ± 0.015	0.880 ± 0.011	0.925 ± 0.007	0.571 ± 0.004	10.6
Encoder Convolutions							
First conv							
FP	0.651 ± 0.004	0.840 ± 0.076	0.528 ± 0.019	0.867 ± 0.017	0.922 ± 0.011	0.574 ± 0.004	10.6
Int8	0.657 ± 0.003	0.825 ± 0.015	0.548 ± 0.003	0.866 ± 0.004	0.925 ± 0.010	0.577 ± 0.001	13.8
Remaining conv							
Bin	0.561 ± 0.036	1.120 ± 0.061	0.281 ± 0.132	0.401 ± 0.022	0.449 ± 0.080	0.247 ± 0.096	15.2
Bin-R	0.653 ± 0.005	1.040 ± 0.018	0.401 ± 0.034	0.811 ± 0.011	0.890 ± 0.007	0.563 ± 0.006	14.5
Spatial Reduction							
Max	0.653 ± 0.005	1.040 ± 0.018	0.401 ± 0.034	0.811 ± 0.011	0.890 ± 0.007	0.563 ± 0.006	14.5
Aver.	0.656 ± 0.003	1.068 ± 0.033	0.354 ± 0.038	0.788 ± 0.027	0.873 ± 0.011	0.558 ± 0.015	13.9
Sub.S.	0.640 ± 0.022	1.128 ± 0.053	0.362 ± 0.024	0.783 ± 0.003	0.881 ± 0.007	0.537 ± 0.015	14.4
Learn	0.648 ± 0.009	0.890 ± 0.066	0.517 ± 0.029	0.848 ± 0.009	0.916 ± 0.003	0.571 ± 0.006	14.2
Early Learn	0.656 ± 0.002	0.943 ± 0.034	0.491 ± 0.024	0.844 ± 0.015	0.906 ± 0.005	0.568 ± 0.002	16.2
Decoder Convolutions							
Remaining convs							
Int8	0.658 ± 0.002	0.964 ± 0.020	0.488 ± 0.030	0.840 ± 0.013	0.900 ± 0.001	0.569 ± 0.002	27.2
BIN-R	0.655 ± 0.003	1.018 ± 0.006	0.451 ± 0.001	0.456 ± 0.001	0.481 ± 0.002	0.329 ± 0.008	30.1
Descriptor conv							
FP	0.652 ± 0.005	0.926 ± 0.022	0.506 ± 0.025	0.853 ± 0.007	0.917 ± 0.003	0.571 ± 0.003	47.2
Int8							

To enable self-supervised training, spatial and non-spatial augmentations for the homography transformation are required. For spatial transformations, we utilize crop, translation, scale, rotation, and symmetric perspective. Non-spatial transformations applied are per-pixel Gaussian noise, Gaussian blur, color augmentation in brightness, contrast, saturation, and hue. Finally, we randomly shuffle the color channels and convert images to gray scale. Please refer to [19] for more details.

B. Designing ZippyPoint

We conduct our DNN quantization investigation on the task of homography estimation. Homography estimation is a commonly used task for the evaluation of self-supervised learned models [1], [39], [19]. With the self-supervised learned models optimized using homography-transformed images, this task eliminates domain shifts due to missing 3D information and provides a simpler benchmark for ablation studies.

We evaluate our method on image sequences from the HPatches dataset [49]. HPatches contains 116 scenes, separated in 57 illumination and 59 viewpoint sequences. Each sequence is comprised of 6 images, with the first image used as a reference. The remaining images are used to form pairs for evaluation. As is common practice, we report Repeatability (Repeat.), Localization Error (Loc), Matching Score (M.Score), and Homography Accuracy with thresholds of 1, 3 and 5 pixels (Cor-1, Cor-3, Cor-5). We additionally benchmark and report the CPU speeds in Frames Per Seconds (FPS) on an Apple M1 ARM processor.

Baseline We initiate our investigation in Table I from a re-implementation of the KP2D architecture, however, we make some minor modifications to enable a structured search with minimal macro-block interference. Specifically, KP2D uses a shortcut connection between the encoder and decoder macro-blocks. We remove this skip-connection to constrain the

interaction between two macro-blocks to a single point. Furthermore, we replace the leaky ReLUs with hard-swish [32], a comparable but faster alternative. The results in *Baseline* are comparable to KP2D, while our baseline model runs slightly faster.

We partition our baseline architecture into five macro-blocks. These include the first encoder convolution, the remaining encoder convolutions, spatial reduction (e.g., pooling) layers, the non-head decoder convolutions, and the head decoder convolutions, as depicted in Fig. 2 by the five different colours.

Macro-Block I: First Encoder Convolution For macro-block I, we considered two configurations: FP and INT8. Although [11], [12] suggest that keeping the first convolution in FP has a negligible effect on application throughput while degradation of functional performance is observed with lower precision, our findings suggest otherwise. Specifically, we find that using an INT8 convolution improves throughput by as much as 3 FPS, while having no detectable impact on functional performance. We ascribe this to the fact that the input images are also represented in INT8. Therefore, discretization of the input sequence does not cause a loss of information, while enabling the use of a more efficient INT8 convolution.

Macro-Block II: Encoder Convolutions For the encoder convolutions, we considered three configurations: INT8, binary (BIN), and binary with a high-precision residual (BIN-R). While using BIN convolutions in the encoder significantly improves application throughput, functional performance is severely hindered, as measured by the halving of correctness metrics. This drop is consistent with findings in the literature for semantic segmentation [50] while conflicting with image-level classification experiments [11]. This further advocated for the importance of task-specific investigations.

TABLE II: We evaluate the efficacy of different normalization layers when combined with Sigmoid. We find that the binary descriptor normalization layer consistently improves all metrics.

	Norm	Repeat. \uparrow	Loc. \downarrow	Cor-1 \uparrow	Cor-3 \uparrow	Cor-5 \uparrow	M.Score \uparrow
Full Precision	L_2	0.644 ± 0.003	0.788 ± 0.005	0.580 ± 0.007	0.886 ± 0.008	0.933 ± 0.010	0.569 ± 0.003
Sigmoid		0.640 ± 0.005	0.809 ± 0.049	0.173 ± 0.300	0.285 ± 0.493	0.305 ± 0.528	0.187 ± 0.318
Sigmoid + $\ L_2\$	L_2	0.650 ± 0.001	0.803 ± 0.010	0.491 ± 0.015	0.822 ± 0.009	0.888 ± 0.003	0.513 ± 0.003
Sigmoid + Bin.Norm (Ours)	Bin.Norm	0.651 ± 0.003	0.796 ± 0.016	0.545 ± 0.005	0.880 ± 0.090	0.925 ± 0.004	0.553 ± 0.002

TABLE III: We compare ZippyPoint with full precision or binary descriptors against state-of-the-art methods. ZippyPoint performs on par with other full-precision methods, while running $5\times$ faster than the remaining learned methods. When compared to binary hand-crafted methods, ZippyPoint consistently outperforms all other methods, often by a large margin.

	Repeat. \uparrow	Loc. \downarrow	Cor-1 \uparrow	Cor-3 \uparrow	Cor-5 \uparrow	M.Score \uparrow
Full-Precision Descriptors						
SuperPoint [1]	0.631	1.109	0.491	0.833	0.893	0.318
SIFT [7]	0.451	0.855	0.622	0.845	0.878	0.304
SURF [8]	0.491	1.150	0.397	0.702	0.762	0.255
KP2D [19]	0.686	0.890	0.591	0.867	0.912	0.544
ZippyPoint (Ours)	0.652 ± 0.005	0.926 ± 0.022	0.506 ± 0.025	0.853 ± 0.007	0.917 ± 0.003	0.571 ± 0.003
Binary Descriptors						
BRISK [4]	0.566	1.077	0.414	0.767	0.826	0.258
ORB [6]	0.532	1.429	0.131	0.422	0.540	0.218
ZippyPoint (Ours)	0.652 ± 0.005	0.926 ± 0.022	0.433 ± 0.007	0.820 ± 0.007	0.887 ± 0.006	0.571 ± 0.003

To alleviate such drastic performance drops, we introduce high precision INT8 representations in the form of a residual operation. For convolutional operations with a mismatch in the number of channels, we introduce additional INT8 1×1 convolutions on the residual path. This ensures the high-precision paths maintain their INT8 precision, while matching the channel dimensions. The additional high-precision INT8 residuals improve performance significantly. This once again advocates for the redundancy of FP representation in the encoder, as the encoder is not bottlenecked by INT8 precision.

Macro-Block III: Spatial Reduction For the spatial reduction layers, we considered four configurations: average-pooling (Aver.), max-pooling (Max), sub-sampling (Sub.S.) and a learned projection having the same kernel size and striding as the original pooling layers (Learn). As common in DNNs, our baseline implementation utilizes max-pooling, however, max-pool in QNNs favours saturation regimes which eliminate information in low-precision features [11]. Using instead average pooling further degrades the performance. This is attributed to the errors introduced due to the roundings and truncations, essential for integerized arrays. To further highlight this error, a simple Sub-Sampling that only uses information from a quarter of the kernel window yields comparable performance to average-pool.

To alleviate the challenges highlighted above, we propose the use of a learned pooling operation. The learned pooling comes in the form of an INT8 convolutional operation with the same kernel size and stride as the pooling operations. We select INT8 so as to maintain the representational precision of the network, as defined by the macro-block I and the high precision residuals.

While operating at a comparable run-time to max pooling, the performance metrics are significantly improved. This further corroborates our hypothesis that learned pooling can

address both the aforementioned challenges. Finally, we investigate the effect of the pooling placement. We change the location of the pooling operations from the end to the beginning of each convolutional block. While with FP convolutional layers this would cause a $4\times$ speedup for each convolution, in quantized convolutions the gain is even greater [46].

Macro-Block IV: Decoder Convolutions For the decoder convolutions, we considered two configurations: INT8, and BIN-R. We do not investigate BIN due to the large performance drop observed in macro-block II. Unlike the findings from macro-block II, our decoder experiments demonstrate the importance of INT8. These findings highlight the benefits of mixed-precision networks. Selecting INT8 for the entire network would not yield the best possible throughput, as seen by the choice of BIN-R in the encoder. In addition, using BIN-R for the entire network would not yield a high functional performance.

Macro-Block V: Final Decoder Convolutions For the final convolutions, we considered either FP and INT8 for the score, location, and descriptor heads independently. We find that score and location heads require FP representations, with models often completely failing to optimize otherwise. On the other hand, the descriptor branch can be optimized with INT8, significantly improving the throughput.

Overall Network Quantization To summarize our findings. First, latency can be significantly improved when quantizing the first and last convolutional layers to INT8, while having an insignificant effect on functional performance. This is contrary to findings from prior work [11], [12]. Second, the best performance was achieved with the use of a mixed-precision network. A network comprised only of BIN-R or INT8 convolutions would yield sub-optimal results. This observation suggests that good quality, general-purpose features can be extracted using skip-connections and

TABLE IV: Comparison of the average visual localization accuracy vs descriptor matching speed between two images on AachenV1.1 Day-Night. ZippyPoint consistently outperforms all other binary methods.

	Day \uparrow	Night \uparrow	FPS \uparrow
Full-Precision Descriptors			
SuperPoint [1]	92.8	79.6	24.4
SIFT [7]	90.3	58.8	34.5
Binary Descriptors			
BRISK [4]	83.7	32.5	70.4
ORB [6]	37.1	1.7	334.5
ZippyPoint (Ours)	87.1	64.7	334.5

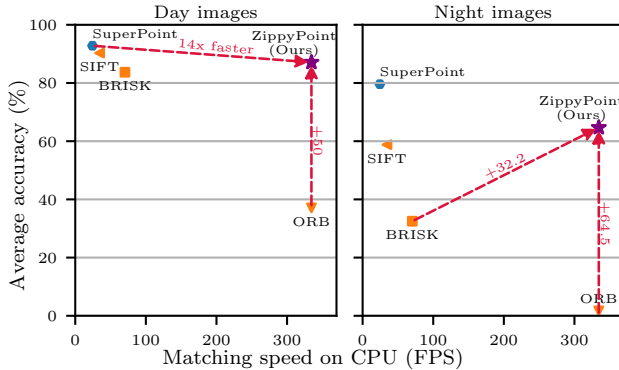


Fig. 3: Comparison of the average visual localization accuracy vs descriptor matching speed between two images on AachenV1.1 Day-Night.

low-precision convolutions. At the same time, it suggests that dense task predictors benefit from higher precision to properly reconstruct the target information from the encoded features. Third, we observe that the prediction heads for regression tasks (score and location) cannot be quantized and should be left in FP, while the descriptor head can be quantized to INT8. This further drives the importance of the structured investigation, like the layer partitioning and traversal strategy.

Binarizing descriptors We initiate the descriptor exploration using sigmoid as a soft approximation for every bit [16], [51], and the hamming triplet loss proposed by [16]. Table II demonstrates a significant performance drop compared to the baseline, with large reported variance, in particular for the correctness metric. We conjecture that this spans from the lack of a normalization layer, that causes the sigmoid to saturate, yielding uninformative gradients. To test this assumption, we append an $\|L_2\|$ normalization layer after the element-wise sigmoid operation. This constrains the activations, and as seen experimentally, dramatically improves performance and reduces the variance, yielding a more stable optimization process.

In this paper we hypothesize that analogous to $\|L_2\|$ normalization for vectors in metric learning, we can optimize using a binary normalization layer by setting the number of bits constant (Sec. III-C). Using the proposed binary normalization layer closes the gap in functional performance when compared to the full precision descriptors, while significantly reducing descriptor storage requirements. Note that, during

inference, one can simply replace the optimization objective and set to 1 the top-k logits.

Comparison to state-of-the-art We compare ZippyPoint with state-of-the-art methods in Table III. For a fair comparison, we group methods given the descriptor precision. In full-precision, we can see that ZippyPoint performs on par with other methods. In particular, it consistently outperforms SuperPoint and compares favourably to KP2D. Meanwhile, the throughput gain is almost $5\times$. We refrain from comparing the run-time to hand-crafted methods due to differences in algorithmic optimization efforts by the community.

The benefit of our ZippyPoint shines when comparing binary descriptor methods, the combination of the fast architecture from Table I and the binary optimization strategy from Table II. As it can be seen, we consistently outperform ORB [18] by a large margin in all metrics. We additionally outperform BRISK [4] in all metrics and even report double the matching score, a crucial metric for adaptation of these methods in downstream tasks like visual localization.

C. Visual Localization

Camera localization is one of the key applications of local feature descriptors in images. Many visual systems, such as mobile robots, rely on accurate camera localization. Both relative [52] and absolute camera [53] localization require good local feature descriptors to match. We evaluate trained descriptors on camera localization, to further test the generalization capability of the approach on images with transformation domains other than homography. Following recent literature [24], [2], we measure the performance of absolute camera localization. In particular, we use the hloc framework [54], similar to [24], and directly evaluate on the challenging Aachen Day-Night dataset from the visual localization benchmark [10], [55].

Table IV and Fig. 3 present the average localization accuracy, and the associated speed for matching two images, in FPS. While SuperPoint and ZippyPoint generate the same number of keypoints, and the performance during day is comparable, the matching is $14\times$ faster. This is attributed to the more efficient similarity comparison that can be computed due to the binary descriptors. Localization of ZippyPoint during night is inferior to SuperPoint, however, we expect optimization of the image transformations during training can close this gap further.

Compared to ORB, ZippyPoint consistently outperformed by a large margin at a comparable matching speed. BRISK on the other hand, is competitive to ours on the day dataset, with the slower run-time of BRISK attributed to the larger descriptor size, twice that of ZippyPoint, and the increased number of detected keypoints. However, the more challenging night dataset paints a different picture, with ZippyPoint outperforming BRISK by 32.2%. This further attests to the need for efficient learned detection and description networks.

V. CONCLUSION

In this paper, we investigated efficient detection and description of learned local image points through mixed-

precision quantization of network components and binarization of descriptors. To that end, we follow a structured investigation we refer to as layer partitioning and traversal for the quantization of the network. In addition, we propose the use of a binary normalization layer, to generate length invariant binary descriptors.

We obtained a $5\times$ throughput improvement with minor degradation of descriptor performance. In addition, we find that the binary normalization layer allows the network to operate on par with full-precision networks, while consistently outperforming hand-crafted binary descriptor methods. The results show the suitability of our approach to challenging downstream tasks such as visual localization. We believe that further research in this direction could in the future result in a truly powerful binary descriptor method, useful in several real-time robotic applications.

REFERENCES

- [1] D. DeTone, T. Malisiewicz, and A. Rabinovich, "Superpoint: Self-supervised interest point detection and description," in *CVPRW*, 2018.
- [2] M. Dusmanu et al., "D2-net: A trainable cnn for joint description and detection of local features," in *CVPR*, 2019.
- [3] P.-E. Sarlin, D. DeTone, T. Malisiewicz, and A. Rabinovich, "SuperGlue: Learning feature matching with graph neural networks," in *CVPR*, 2020.
- [4] S. Leutenegger, M. Chli, and R. Y. Siegwart, "Brisk: Binary robust invariant scalable keypoints," in *ICCV*, 2011.
- [5] M. Calonder, V. Lepetit, C. Strecha, and P. Fua, "Brief: Binary robust independent elementary features," in *ECCV*, 2010.
- [6] E. Rublee, V. Rabaud, K. Konolige, and G. Bradski, "Orb: An efficient alternative to sift or surf," in *ICCV*, 2011.
- [7] D. G. Lowe, "Distinctive image features from scale-invariant keypoints," *IJCV*, vol. 60, no. 2, pp. 91–110, 2004.
- [8] H. Bay, T. Tuytelaars, and L. V. Gool, "Surf: Speeded up robust features," in *ECCV*, 2006.
- [9] J. Heinly, E. Dunn, and J.-M. Frahm, "Comparative evaluation of binary features," in *ECCV*, 2012.
- [10] T. Sattler et al., "Benchmarking 6dof outdoor visual localization in changing conditions," in *CVPR*, 2018.
- [11] M. Rastegari, V. Ordonez, J. Redmon, and A. Farhadi, "Xnor-net: Imagenet classification using binary convolutional neural networks," in *ECCV*, 2016.
- [12] Z. Liu et al., "Bi-real net: Enhancing the performance of 1-bit cnns with improved representational capability and advanced training algorithm," in *ECCV*, 2018.
- [13] J. Bethge, H. Yang, M. Bornstein, and C. Meinel, "Back to simplicity: How to train accurate bnns from scratch?" *arXiv*, 2019.
- [14] G. P. Leonardi and M. Spallanzani, "Analytical aspects of non-differentiable neural networks," *arXiv*, 2020.
- [15] F. Shen, Y. Xu, L. Liu, Y. Yang, Z. Huang, and H. T. Shen, "Unsupervised deep hashing with similarity-adaptive and discrete optimization," *T-PAMI*, vol. 40, no. 12, pp. 3034–3044, 2018.
- [16] H. Lai, Y. Pan, Y. Liu, and S. Yan, "Simultaneous feature learning and hash coding with deep neural networks," in *CVPR*, 2015.
- [17] J. L. Schonberger and J.-M. Frahm, "Structure-from-motion revisited," in *CVPR*, 2016.
- [18] R. Mur-Artal, J. M. M. Montiel, and J. D. Tardos, "Orb-slam: a versatile and accurate monocular slam system," *IEEE T-RO*, vol. 31, no. 5, pp. 1147–1163, 2015.
- [19] J. Tang, H. Kim, V. Guizilini, S. Pillai, and R. Ambrus, "Neural outlier rejection for self-supervised keypoint learning," in *ICLR*, 2020.
- [20] E. Tola, V. Lepetit, and P. Fua, "Daisy: An efficient dense descriptor applied to wide-baseline stereo," *T-PAMI*, vol. 32, no. 5, pp. 815–830, 2009.
- [21] C. B. Choy, J. Gwak, S. Savarese, and M. Chandraker, "Universal correspondence network," in *NIPS*, 2016.
- [22] M. E. Fathy, Q.-H. Tran, M. Z. Zia, P. Vernaza, and M. Chandraker, "Hierarchical metric learning and matching for 2d and 3d geometric correspondences," in *ECCV*, 2018.
- [23] Y. Ono, E. Trulls, P. Fua, and K. M. Yi, "Lf-net: Learning local features from images," *NIPS*, 2018.
- [24] J. Revaud et al., "R2d2: repeatable and reliable detector and descriptor," in *NIPS*, 2019.
- [25] K. Lin, J. Lu, C.-S. Chen, and J. Zhou, "Learning compact binary descriptors with unsupervised deep neural networks," in *CVPR*, 2016.
- [26] F. Shen, C. Shen, W. Liu, and H. Tao Shen, "Supervised discrete hashing," in *CVPR*, 2015.
- [27] J. Wang, T. Zhang, N. Sebe, H. T. Shen, et al., "A survey on learning to hash," *T-PAMI*, vol. 40, no. 4, pp. 769–790, 2017.
- [28] M. Norouzi, D. J. Fleet, and R. R. Salakhutdinov, "Hamming distance metric learning," *NIPS*, 2012.
- [29] K. Musgrave, S. Belongie, and S.-N. Lim, "A metric learning reality check," in *ECCV*, 2020.
- [30] S. Gould, R. Hartley, and D. J. Campbell, "Deep declarative networks," *T-PAMI*, 2021.
- [31] K. He and J. Sun, "Convolutional neural networks at constrained time cost," in *CVPR*, 2015.
- [32] A. Howard et al., "Searching for mobilenetv3," in *ICCV*, 2019.
- [33] X. Zhang, J. Zou, K. He, and J. Sun, "Accelerating very deep convolutional networks for classification and detection," *T-PAMI*, vol. 38, no. 10, pp. 1943–1955, 2015.
- [34] A. Obukhov, M. Rakhuba, S. Georgoulis, M. Kanakis, D. Dai, and L. Van Gool, "T-basis: a compact representation for neural networks," in *ICML*, 2020.
- [35] A. Obukhov et al., "Spectral tensor train parameterization of deep learning layers," in *AISTATS*, 2021.
- [36] B. Jacob et al., "Quantization and training of neural networks for efficient integer-arithmetic-only inference," in *CVPR*, 2018.
- [37] K. Simonyan and A. Zisserman, "Very deep convolutional networks for large-scale image recognition," *arXiv*, 2014.
- [38] A. L. Maas, A. Y. Hannun, A. Y. Ng, et al., "Rectifier nonlinearities improve neural network acoustic models," in *Proc. icml*, vol. 30, no. 1. Citeseer, 2013, p. 3.
- [39] P. H. Christiansen, M. F. Kragh, Y. Brodskiy, and H. Karstoft, "Unsuperpoint: End-to-end unsupervised interest point detector and descriptor," *arXiv*, 2019.
- [40] R. Hadsell, S. Chopra, and Y. LeCun, "Dimensionality reduction by learning an invariant mapping," in *CVPR*, 2006.
- [41] K. Q. Weinberger and L. K. Saul, "Distance metric learning for large margin nearest neighbor classification," *JMLR*, vol. 10, no. 2, 2009.
- [42] J. Deng, J. Guo, N. Xue, and S. Zafeiriou, "Arcface: Additive angular margin loss for deep face recognition," in *CVPR*, 2019.
- [43] B. Amos, V. Koltun, and J. Z. Kolter, "The limited multi-label projection layer," *arXiv*, 2019.
- [44] B. Amos and J. Z. Kolter, "Optnet: Differentiable optimization as a layer in neural networks," in *ICML*, 2017.
- [45] M. A. et al., "TensorFlow: Large-scale machine learning on heterogeneous systems," 2015, software available from tensorflow.org. [Online]. Available: <https://www.tensorflow.org/>
- [46] L. Geiger et al., "Larq: An open-source library for training binarized neural networks," *Journal of Open Source Software*, vol. 5, no. 45, p. 1746, Jan. 2020.
- [47] T.-Y. Lin et al., "Microsoft coco: Common objects in context," in *ECCV*, 2014.
- [48] D. P. Kingma and J. Ba, "Adam: A method for stochastic optimization," *arXiv*, 2014.
- [49] V. Balntas, K. Lenc, A. Vedaldi, and K. Mikolajczyk, "Hpatches: A benchmark and evaluation of handcrafted and learned local descriptors," in *CVPR*, 2017.
- [50] B. Zhuang, C. Shen, M. Tan, L. Liu, and I. Reid, "Structured binary neural networks for accurate image classification and semantic segmentation," in *CVPR*, 2019.
- [51] W. Liu, J. Wang, R. Ji, Y.-G. Jiang, and S.-F. Chang, "Supervised hashing with kernels," in *CVPR*, 2012.
- [52] D. Nistér, "An efficient solution to the five-point relative pose problem," *T-PAMI*, vol. 26, no. 6, pp. 756–770, 2004.
- [53] L. Kneip, D. Scaramuzza, and R. Siegwart, "A novel parametrization of the perspective-three-point problem for a direct computation of absolute camera position and orientation," in *CVPR*, 2011.
- [54] P.-E. Sarlin, C. Cadena, R. Siegwart, and M. Dymczyk, "From coarse to fine: Robust hierarchical localization at large scale," in *CVPR*, 2019.
- [55] T. Sattler, T. Weyand, B. Leibe, and L. Kobbelt, "Image retrieval for image-based localization revisited," in *BMVC*, 2012.